PLOS ONE

RESEARCH ARTICLE

Metabolic engineering considerations for the heterologous expression of xylose-catabolic pathways in *Saccharomyces cerevisiae*

Deokyeol Jeong[1☯], Eun Joong Oh[2☯], Ja Kyong Ko[3], Ju-Ock Nam[1], Hee-Soo Park[1], Yong-Su Jin[4,5], Eun Jung Lee[6]*, Soo Rin Kim[1]*

1 School of Food Science and Biotechnology, Kyungpook National University, Daegu, Republic of Korea, **2** Renewable and Sustainable Energy Institute (RASEI), University of Colorado Boulder, Boulder, Colorado, United States of America, **3** Clean Energy Research Center, Korea Institute of Science and Technology (KIST), Seoul, Republic of Korea, **4** Carl R. Woese Institute for Genomic Biology, University of Illinois at Urbana-Champaign, Urbana, Illinois, United States of America, **5** Department of Food Science and Human Nutrition, University of Illinois at Urbana-Champaign, Urbana, Illinois, United States of America, **6** Department of Chemical Engineering, School of Applied Chemical Engineering, Kyungpook National University, Daegu, Republic of Korea

☯ These authors contributed equally to this work.
* eunjunglee@knu.ac.kr (EJL); soorinkim@knu.ac.kr (SRK)

Citation: Jeong D, Oh EJ, Ko JK, Nam J-O, Park H-S, Jin Y-S, et al. (2020) Metabolic engineering considerations for the heterologous expression of xylose-catabolic pathways in *Saccharomyces cerevisiae*. PLoS ONE 15(7): e0236294. https://doi.org/10.1371/journal.pone.0236294

Editor: Enrico Baruffini, University of Parma, ITALY

Received: March 11, 2020

Accepted: July 1, 2020

Published: July 27, 2020

Peer Review History: PLOS recognizes the benefits of transparency in the peer review process; therefore, we enable the publication of all of the content of peer review and author responses alongside final, published articles. The editorial history of this article is available here: https://doi.org/10.1371/journal.pone.0236294

Data Availability Statement: All relevant data are within the manuscript and its Supporting Information files.

Funding: This work was supported by grants from the National Research Foundation (NRF) of Korea

Abstract

Xylose, the second most abundant sugar in lignocellulosic biomass hydrolysates, can be fermented by *Saccharomyces cerevisiae* expressing one of two heterologous xylose pathways: a xylose oxidoreductase pathway and a xylose isomerase pathway. Depending on the type of the pathway, its optimization strategies and the fermentation efficiencies vary significantly. In the present study, we constructed two isogenic strains expressing either the oxidoreductase pathway (XYL123) or the isomerase pathway (XI-XYL3), and delved into simple and reproducible ways to improve the resulting strains. First, the strains were subjected to the deletion of *PHO13*, overexpression of *TAL1*, and adaptive evolution, but those individual approaches were only effective in the XYL123 strain but not in the XI-XYL3 strain. Among other optimization strategies of the XI-XYL3 strain, we found that increasing the copy number of the xylose isomerase gene (*xylA*) is the most promising but yet preliminary strategy for the improvement. These results suggest that the oxidoreductase pathway might provide a simpler metabolic engineering strategy than the isomerase pathway for the development of efficient xylose-fermenting strains under the conditions tested in the present study.

Introduction

Global climate change has accelerated efforts to find eco-friendly alternatives for fossil fuels. One idea is to use wood wastes and agricultural residues called lignocellulosic biomass, which does not interfere with food or the environment [1]. Lignocellulosic biomass, mainly composed of cellulose and hemicellulose, is hydrolyzed into glucose, xylose, and other simple and minor sugars, which can be transformed into biofuels and chemicals by microbial fermentation [2].

funded by the Korea government (NRF-2018R1A2B2007426). This work was also supported by the National Research Foundation of Korea (NRF) grant funded by the Korea government (MSIT) (No. 2019R1F1A1062633).

Competing interests: The authors have declared that no competing interests exist.

The yeast *Saccharomyces cerevisiae* is an industrial microorganism with superior sugar fermentation capabilities and stress tolerance. However, this yeast cannot metabolize xylose, requiring the introduction of a heterologous xylose pathway [3,4] as summarized in Fig 1A. The first step is to introduce either the NAD(P)H-specific xylose reductase/NAD^+-specific xylitol dehydrogenase (oxidoreductase, XR/XDH) pathway derived from *Pichia stipitis* or the xylose isomerase (XI) pathway derived from various anaerobic microorganisms, both of which convert xylose to xylulose. Next, xylulose is converted into xylulose-5-phosphate by xylulokinase either by endogenous but overexpressed *S. cerevisiae XKS1* or *P. stipitis XYL3*. Finally, xylulose-5-phosphate is metabolized into ethanol through the native pentose phosphate (PP) pathway connected to glycolysis in *S. cerevisiae*. In engineered strains of *S. cerevisiae* expressing the xylose oxidoreductase pathway, the rate of xylose consumption and ethanol productivity are relatively high, but xylitol, glycerol, and acetate are accumulated as byproducts [3,5]. This byproduct accumulation is mainly due to an unbalanced cofactor preference of the xylose oxidoreductase pathway, leading to a shortage of NAD^+ [3]. On the other hand, the xylose isomerase pathway is cofactor-independent, the expression of which in *S. cerevisiae* can lead to a high ethanol yield with minimal byproduct accumulation even under anaerobic conditions [6]. However, slow growth and xylose consumption were commonly observed in the engineered *S. cerevisiae* strains expressing the xylose isomerase pathway compared to those expressing xylose oxidoreductase pathway [5,7,8].

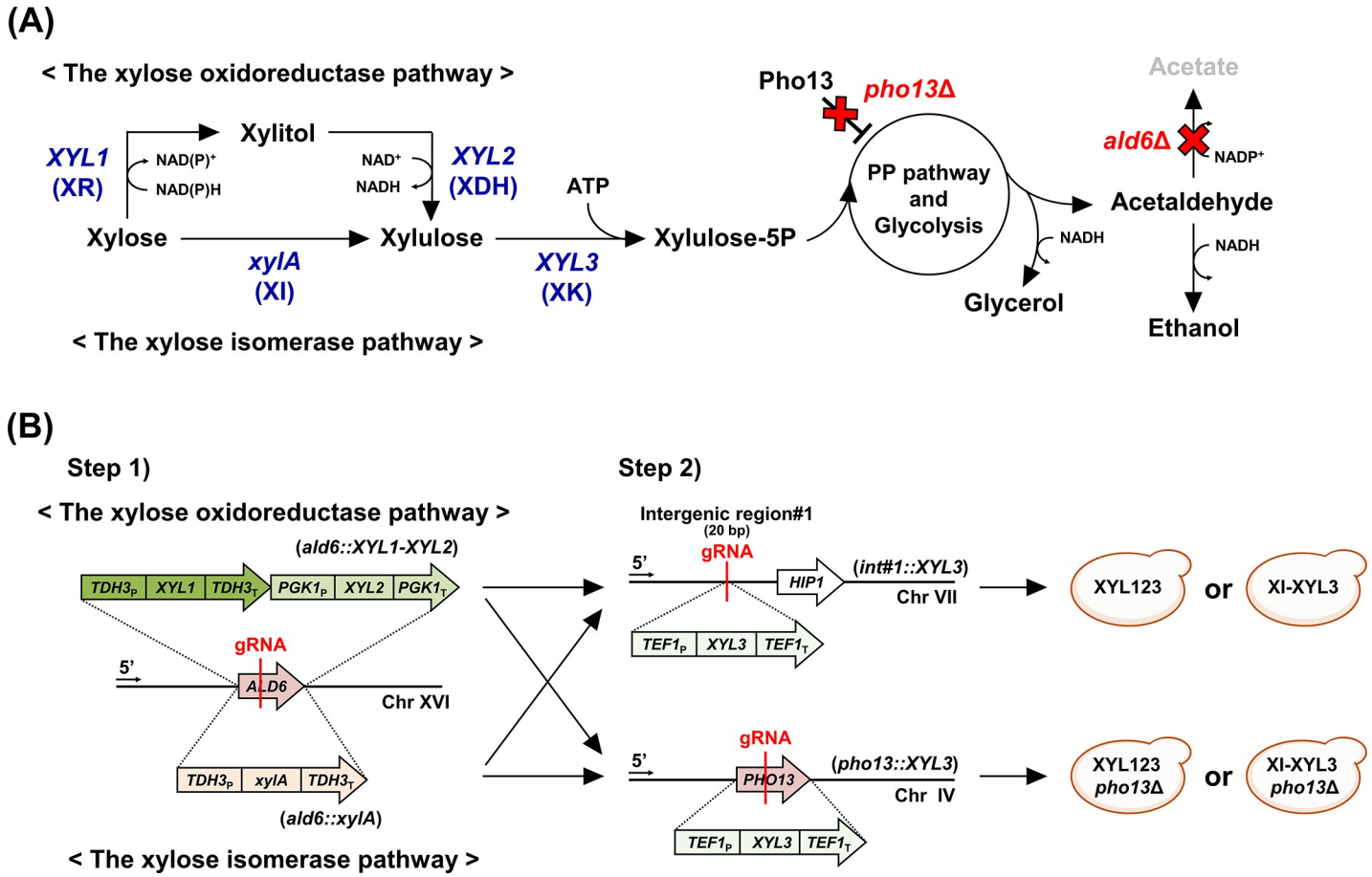

Fig 1. Construction of isogenic *S. cerevisiae* strains expressing a different type of xylose pathways. (A) Two different xylose pathways. (B) Strain construction using a precise Cas9-based genome integration strategy.

https://doi.org/10.1371/journal.pone.0236294.g001

Adaptive evolution have been the most commonly used and the most effective approach to improve both the strains expressing the oxidoreductase pathway [3,9,10] and the strains expressing the isomerase pathway [11–13]. Some of the evolved strains were subjected to genome sequencing to identify genetic changes responsible for the improved phenotypes. In prior studies, the loss of function mutation of the *PHO13* gene encoding phosphatase with a broad substrate spectrum was identified as a key mutation of an evolved strain expressing the xylose oxidoreductase pathway [3,14,15]. Deletion of the *PHO13* gene (*pho13*Δ) now provides simple, effective, and transferrable to different strain backgrounds expressing the xylose oxidoreductase pathway [3,14–16]. Moreover, it was further confirmed that *pho13*Δ leads to transcriptional and metabolic shifts toward efficient xylose fermentation [17,18]. However, it has not been clearly understood how strains expressing the isomerase pathway can be simply improved, although there have been several attempts of genome sequencing of the evolved strains expressing the isomerase pathway [19–24].

In this study, we constructed two isogenic strains expressing either the xylose oxidoreductase pathway or the xylose isomerase pathway through a precise Cas9-based genome integration strategy [25,26]. Deletion of the *PHO13* gene, adaptive evolution, the upregulation of the PP pathway, and some other strategies were performed to identify the most critical and simple factor to improve the strain expressing the xylose isomerase pathway.

Materials and methods

Culture conditions

The *S. cerevisiae* strains were routinely grown on yeast extract-peptone (YP) medium (10 g/L yeast extract, 20 g/L peptone) containing 20 g/L of glucose (YPD) at 30˚C for fermentation experiments. The medium used for yeast transformation was YPD agar plate supplemented with antibiotics (100 μg/mL nourseothricin sulfate, 300 μg/mL hygromycin B, 300 μg/mL G418 sulfate). *Escherichia coli* TOP10 (Invitrogen, Carlsbad, CA, USA) was used to amplify plasmid DNA. *E. coli* was cultured in Luria-Bertani (LB) medium (5 g/L yeast extract, 10 g/L tryptone, 10 g/L NaCl) at 37˚C and, if necessary, 100 μg/mL ampicillin (LBA) or 50 μg/mL kanamycin (LBK) was added.

Plasmid construction and strain engineering

The strains and plasmids used in this study are summarized in Table 1 and S1 Table, respectively. The detailed materials and methods for plasmid and strain construction are available in the online supplementary information (S1 Text).

Flask fermentation experiments

After pre-cultivation in YP medium with 20 g/L of glucose for 24 hours at 250 rpm, yeast cells were harvested by centrifugation at 3,134 ×g, at 4˚C for 5 min, and washed with distilled water. The initial cell concentration was adjusted to an optical density at 600 nm (OD_{600}) of 1.0 or 50.0, which corresponds to initial cell density of 0.5 and 25 g DCW/L, respectively, and the cell pellet was inoculated into 20 mL of YP medium containing 40 g/L xylose. Oxygen-limited cultivation was performed at 30˚C in a 100-mL Erlenmeyer flask using a rotary shaker at 80 rpm. Anaerobic cultivation was performed at 30˚C in 125-mL serum bottles using a rotary shaker at 130 rpm. To remove oxygen, the serum bottles were flushed with nitrogen that had passed through a heated, reduced copper column. All experiments were performed in biological triplicate.

Table 1. *Saccharomyces cerevisiae* strains used in this study.

Strains	Description/relevant genotype	Reference
D452-2	*Matα leu2 his3 ura3*	[27]
XYL12	D452-2 *ald6*::$TDH3_P$-*XYL1*-$TDH3_T$-$PGK1_P$-*XYL2*[1)]-$PGK1_T$	This study
XYL123	XYL12 *int#1*::$TEF1_P$-*XYL3*-$TEF1_T$; DY01	[25]
XYL123 *pho13*Δ	XYL12 *pho13*::$TEF1_P$-*XYL3*-$TEF1_T$; DY02	[25]
XYL123e	XYL123 evolved in 40 g/L xylose	This study
XI	D452-2 *ald6*::$TDH3_P$-*xylA*-$TDH3_T$	This study
XI-XYL3	XI *int#1*::$TEF1_P$-*XYL3*-$TEF1_T$	This study
XI-XYL3 *pho13*Δ	XI *pho13*::$TEF1_P$-*XYL3*-$TEF1_T$	This study
XI-XYL3 *TAL1*	XI-XYL3 with insertion of a *TEF2* promoter in front of *TAL1* gene	This study
XI-XYL3e	XI-XYL3 evolved in 100 g/L xylose	This study
XI-XYL3 *pho13*Δe	XI-XYL3 *pho13*Δ evolved in 100 g/L xylose	This study
XI-XYL3 *gre3*Δ	XI-XYL3 *gre3*::*KanMX*	This study
XI-XYL3 *sor1*Δ	XI-XYL3 with *SOR1* deletion	This study
$(XI)_2$-XYL3	XI-XYL3 *int#6*::$TDH3_P$-*xylA*-$TDH3_T$	This study
XI-$(XYL3)_2$	XI-XYL3 *int#9*::$TEF1_P$-*XYL3*-$TEF1_T$	This study
$(XI)_2$-XYL3 *pho13*Δ	XI-XYL3 *int#6*::$TDH3_P$-*xylA*-$TDH3_T$	This study
δ(XI)-XYL3	XI-XYL3 *leu2*::*LEU2* pYS-δXI	This study
δ(XI)-XYL3 *pho13*Δ	XI-XYL3 *leu2*::*LEU2* pYS-δXI with *PHO13* deletion	This study

XYL1, *XYL2*, and *XYL3* originated from *Pichia stipitis*; *xylA* originated from *Orpinomyces* sp.

https://doi.org/10.1371/journal.pone.0236294.t001

Volumetric growth rate analysis at various xylose concentrations

To compare growth rate after *PHO13* gene deletion, all strains were pre-cultured in 10 mL of YP medium containing 20 g/L of glucose, and the pre-cultured cells were harvested at mid-exponential phase and inoculated into 3 mL of YP medium containing various concentrations of xylose after washing twice with sterilized water. Growth rate analysis was performed in 14-mL Round-Bottom Tubes (SPL, Pocheon, Korea) at 30˚C and 250 rpm with a low initial cell density (0.5 g DCW/L). The control (XYL123 and XI-XYL3) and *pho13*Δ (XYL123 *pho13*Δ and XI-XYL3 *pho13*Δ) strains were compared at 1–200 g/L xylose. Volumetric growth rates (g/L-h) were calculated based on the starting and ending points of the exponential phase. All experiments were performed in biological triplicate.

Transcriptional analysis by RT-qPCR

RT-qPCR was performed by extracting RNA from cells of the exponential phase as previously described [18]. All of the strains were grown in YP media containing 20 g/L glucose or 40 g/L xylose. The cDNA solution, prepared from 1 μg of RNA using the ReverTra Ace® qPCR RT Master Mix (TOYOBO, Osaka, Japan), was used directly with primers and iQ™ SYBR Green Supermix (Bio-Rad, Hercules, CA, USA) for quantitative PCR (qPCR). qPCR was performed using a CFX Connect™ Real-Time PCR Detection System (Bio-Rad, Hercules, CA, USA). The primers used for RT-qPCR are described in S2 Table. All of the measurements were performed in three technical replicates for each biological triplicate.

Adaptive laboratory evolution

After pre-cultivation in YP medium containing 20 g/L of glucose for 24 hours at 250 rpm, yeast cells were harvested by centrifugation at 15,928 ×g, at 4˚C for 1 min. The pre-cultured

cells were washed with distilled water, and the cell pellet was inoculated into 20 mL of YP medium containing 40 g/L or 100 g/L xylose under oxygen-limited conditions (80 rpm). The initial cell densities were adjusted to 0.5 g DCW/L. Growth adaption was performed at 30˚C in a 100-mL Erlenmeyer flask using a rotary shaker at 80 rpm. The cells were transferred to fresh medium when they reached exponential phase. The growth adaption was continued for about 90 days. To confirm that the strains had evolved, three independent colonies were isolated from the YPD agar plate and evaluated by fermentation performances under oxygen-limited conditions (80 rpm).

HPLC analysis

Quantitation of xylose, xylitol, glycerol, acetate, and ethanol in the culture was analyzed by a high-performance liquid chromatography (HPLC; Agilent Technologies, 1260 series, USA) equipped with a Rezex-ROA Organic Acid H+ (8%) (150 mm × 4.6 mm) column (Phenomenex Inc., Torrance, CA, USA). Columns were eluted with 0.005 N H_2SO_4 at 50˚C, and the flow rate was set at 0.6 mL/min, as described previously [28]. Acetate was not detected in all fermentations, and the results were omitted from the figures and tables.

Intracellular metabolite extraction and derivatization

Metabolite extraction was carried out with some modification of the previously described method [29]. Briefly, 5 mL of cell cultures at mid-exponential growth phase were quenched by quick injection into 25 mL of 60% (v/v) cold methanol (HEPES, 10 mM; pH 7.1) at -40˚C. The cells were centrifuged at 3,134 ×g at -20˚C for 5 min, then discard supernatant thoroughly. Subsequently, 1 mL of 75% (v/v) boiling ethanol (HEPES, 10 mM; pH 7.1) was added to the quenched cell pellet, then make sure that cell pellet should be suspended well with boiling ethanol solution. The mixture was then vortexed for 30 s in a max force, incubated at 80˚C for 5 min. The cell residues were separated from the extract by centrifugation at 15,928 ×g at 4˚C for 1 min. The supernatant was then vacuum-dried for 5 h using a speed vacuum concentrator (Labconco, Kansas City, MO, USA).

The vacuum-dried samples were derivatized by methoxyamination and trimethylsilylation as previously described with some modifications [29]. For methoxyamination, 40 μL of methoxyamine hydrochloride in pyridine (40 mg/mL; Sigma-Aldrich, St. Louis, MO, USA) was added to the samples and incubated at 30˚C for 90 min. For trimethylsilylation, 40 μL of N-methyl-N-(trimethylsilyl)trifluoroacetamide (Sigma-Aldrich, St. Louis, MO, USA) was added to the samples and incubated at 37˚C for 30 min.

Intracellular metabolite analysis using GC/MS

GC/MS analysis was conducted using an Agilent 6890 GC equipped with an Agilent 5973 MSD as described previously with some modifications [17]. A 1 μL aliquot of derivatized samples was injected into the GC in a split mode (10:1) and separated on an RTX-5Sil MS column (30 m × 0.25 mm, 0.25-μm film thickness; Restek, Bellefonte, PA, USA). The initial oven temperature was set at 75˚C for 1 min, and then ramped at 15˚C/min to a final temperature of 300˚C, held for 2 min. Helium was used as a carrier gas at a constant flow rate of 0.7 mL/min. The temperatures of ion source and transfer line were set at 230˚C and 280˚C, respectively. An electron impact of 70 eV was used for ionization. The mass selective detector was operated in scan mode with a mass range of 50–550 m/z.

Results

Construction and comparison of two isogenic strains expressing xylose oxidoreductase pathway or xylose isomerase pathway

Two isogenic strains expressing either a xylose oxidoreductase pathway (*XYL1-XYL2*) or the xylose isomerase pathway (*xylA*) were constructed as follows (Fig 1B). For the origin of the genes, *XYL1* and *XYL2* from yeast *P. stipitis* [28] and *xylA* from anaerobic fungus *Orpinomyces* sp. (GenBank No. MK335957) were used which are known to have the highest catalytic activities among the same group of enzymes tested [30,31]. Because acetaldehyde dehydrogenase encoded by the *ALD6* gene plays a major role in acetate accumulation [32], and because acetate is detrimental to xylose metabolism of the oxidoreductase strains [3] as well as the isomerase strains [33,34], the *ALD6* gene was often selected as knockout target for xylose strains [35,36]. In the present study, therefore, the xylose pathway genes, *XYL1-XYL2* or *xylA*, were genome-integrated by replacing the *ALD6* gene by a Cas9-based genome integration strategy, resulting in the *XYL12* (*ald6*::*XYL1-XYL2*) and the XI (*ald6*::*xylA*) strains, respectively. Next, the *XYL3* gene encoding xylulokinase, of which overexpression is required for both pathways, was genome-integrated at an intergenic region (int#1, Fig 1B), resulting in the XYL123 and XI-XYL3 strains, respectively.

When fermenting 40 g/L xylose under oxygen-limited conditions with a low initial cell density (0.5 g DCW/L), the resulting strains showed different phenotypes; while the XYL123 strain consumed over 90% xylose and produced ethanol within 72 h (Fig 2A), the XI-XYL3 strain consumed 10% xylose in the same time period and no ethanol was detected (Fig 2B and Table 2). The difference in the rate of xylose metabolism is primarily due to the thermodynamic advantage of the oxidoreductase pathway compared to the isomerase pathway, as previously reported [37]. Ethanol production by the XI-XYL3 strain was only possible to detect under anaerobic conditions with a high initial cell density (25 g DCW/L) (Table 3). The accumulation of significant amount of xylitol by the XI-XYL3 strain (5.0 g/L) compared to the XYL123 strain (0.6 g/L) was likely due to endogenous non-specific xylose reductase activities (Gre3), which is more significant when the rate of xylose metabolism is slow [38].

Effects of the *PHO13* deletion on xylose fermentation by two xylose-metabolizing strains

To determine the effects of *PHO13* deletion, the *XYL3* gene was genome-integrated by replacing the *PHO13* gene of the *XYL12* and XI strains, resulting in the XYL123 *pho13*Δ and XI-XYL3 *pho13*Δ strains (Fig 1B). When 40 g/L of xylose was provided, the XYL123 *pho13*Δ strain consumed xylose completely in 48 h, resulting in the fermentation time being reduced by 33%, and the growth rate being increased by 1.54-fold as compared to those of the XYL123 strain (Fig 2C and 2D). In addition, the XYL123 *pho13*Δ strain exhibited 1.76-fold higher specific ethanol productivity and a 6.33-fold increase in xylitol yield as a by-product, than that seen in the XYL123 strain (Fig 2E and Table 2). These results confirmed that *pho13*Δ improved the xylose fermentation rate in a strain expressing a heterologous xylose oxidoreductase pathway as previously described [3,18,43,44]. However, *pho13*Δ did not affect xylose consumption or by-product yields in the XI-XYL3 strain expressing the xylose isomerase pathway (Fig 2F and Table 2). Under anaerobic conditions with a high initial cell density (25 g DCW/L), *pho13*Δ rather decreased ethanol production by 20% (Table 3).

PHO13 deletion-induced transcriptional and metabolic changes in two xylose-metabolizing strains

It has been reported that *pho13*Δ induces significant changes at both transcriptional and metabolic levels in the strains expressing the xylose oxidoreductase pathway. First, *pho13*Δ increases

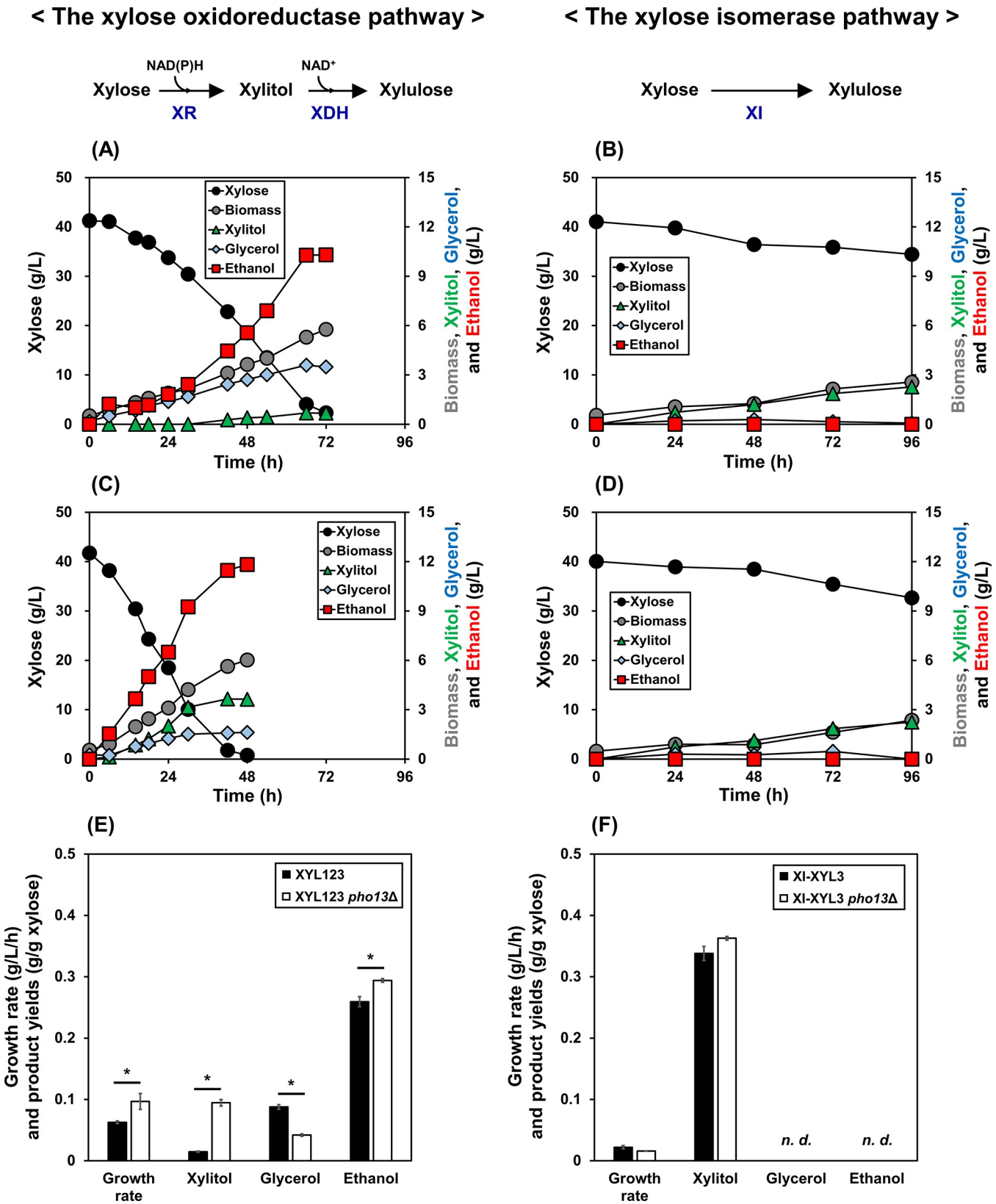

Fig 2. Effect of *PHO13* deletion on xylose fermentation by two xylose-metabolizing strains. (A) The XYL123 strain expressing the xylose oxidoreductase pathway and (B) the XI-XYL3 strain expressing the xylose isomerase pathway were compared to their corresponding *pho13*Δ mutants (C and D, respectively).

(E, F) Volumetric growth rates (g/L-h) and product yields (g/g) of the xylose fermentations. Fermentations were performed in YP medium containing 40 g/L xylose under oxygen-limited conditions (80 rpm), with a low initial cell density (0.5 g DCW/L). Asterisks denote statistically significant differences (Student's t-test, $p < 0.05$). *n. d.*; Not detected.

https://doi.org/10.1371/journal.pone.0236294.g002

the expression levels of *TAL1*, which encodes sedoheptulose-7-phosphate:D-glyceraldehyde-3-phosphate transaldolase in the PP pathway, under both glucose [18,39] and xylose conditions [18], which was confirmed in the XYL123 strain of the present study as well (Fig 3A). Also, *pho13*Δ leads to the reduction in intracellular sedoheptulose-7-phosphate (S7P) and sedoheptulose levels during xylose metabolism [17], as confirmed in Fig 3B. However, in the XI-XYL3 strain, the *TAL1* activation by *pho13*Δ was observed only under glucose conditions (7.3-fold increase, Fig 3A) but not under xylose conditions. Moreover, S7P was not accumulated in the XI-XYL3 strain during xylose metabolism (Fig 3B). Therefore, it was concluded that *pho13*Δ does not contribute to xylose metabolism of the XI-XYL3 strain neither at the transcription levels nor at the metabolic levels under the conditions we tested. It is hypothesized that some metabolic conditions are required for *PHO13* deletion-induced transcriptional activation of *TAL1*, which is independent from the type of a metabolizing sugar. Because the XI-XYL3 strain metabolizes xylose very slowly, a lack of ATP and/or a low level of some metabolic intermediates could be associated with undesirable conditions for the *TAL1* activation.

Adaptive evolution of two xylose-metabolizing strains

Concentration of xylose higher than 10 g/L inhibits the growth of *S. cerevisiae* strains expressing a xylose oxidoreductase pathway, which provides driving force for adaptive evolution as described previously [3]. The XYL123 strains constructed in the present study also showed decrease in the growth rates when the xylose concentration exceeded 10 g/L (Fig 4A). Also, when the XYL123 strain was subjected to serial sub-cultures on 40 g/L xylose, gradual increase in the growth rate of the culture was observed, suggesting the progress of adaptive evolution (Fig 4C). In fact, some selected mutants isolated from the evolved cultures showed improved xylose fermentation capabilities that were comparable to the XYL123 *pho13*Δ strain (S1 and S2 Figs and S3 Table). It is interesting to note that the growth of the XYL123 *pho13*Δ strain was

Table 2. Fermentation profiles of engineered *S. cerevisiae* expressing heterologous xylose fermentation pathways.

Strain	Growth rate (g/L-h)	Xylose consumed (g/L)	Xylose consumption rate (g/L-h)	Product titers (g/L)			$Y_{Xylitol}$	$Y_{Glycerol}$	$Y_{Ethanol}$	$P_{Ethanol}^{*}$
				Xylitol	Glycerol	Ethanol				
XYL123	0.06 ± 0.00	39.9 ± 1.0	0.53 ± 0.02	0.6 ± 0.2	3.3 ± 0.1	10.6 ± 0.4	0.01 ± 0.00	0.09 ± 0.01	0.26 ± 0.01	0.06 ± 0.01
XYL123 *pho13*Δ	0.10 ± 0.01	41.1 ± 1.4	0.93 ± 0.04	3.7 ± 0.2	1.6 ± 0.4	11.9 ± 0.5	0.09 ± 0.01	0.04 ± 0.01	0.29 ± 0.01	0.10 ± 0.01
XI-XYL3	0.04 ± 0.01	14.7 ± 0.5	0.06 ± 0.00	5.0 ± 0.3	*n. d.*	*n. d.*	0.34 ± 0.01	*n. d.*	*n. d.*	*n. d.*
XI-XYL3 *pho13*Δ	0.03 ± 0.00	15.1 ± 1.2	0.07 ± 0.00	5.8 ± 0.1	*n. d.*	*n. d.*	0.36 ± 0.00	*n. d.*	*n. d.*	*n. d.*
$(XI)_2$-XYL3	0.08 ± 0.01	23.2 ± 1.5	0.10 ± 0.01	6.7 ± 0.1	*n. d.*	*n. d.*	0.29 ± 0.02	*n. d.*	*n. d.*	*n. d.*
$(XI)_2$-XYL3 *pho13*Δ	0.06 ± 0.01	21.0 ± 1.0	0.09 ± 0.01	7.8 ± 0.4	*n. d.*	*n. d.*	0.37 ± 0.00	*n. d.*	*n. d.*	*n. d.*
δ(XI)-XYL3	0.10 ± 0.01	27.7 ± 0.2	0.15 ± 0.01	10.5 ± 0.2	0.4 ± 0.1	1.0 ± 0.0	0.34 ± 0.01	0.07 ± 0.00	0.16 ± 0.01	< 0.00
δ(XI)-XYL3 *pho13*Δ	0.11 ± 0.01	32.0 ± 0.6	0.16 ± 0.00	9.2 ± 0.5	*n. d.*	1.6 ± 0.0	0.29 ± 0.00	*n. d.*	0.20 ± 0.01	< 0.00

All strains were cultured in YP medium containing 40 g/L xylose under oxygen-limited conditions (80 rpm) with a low initial cell density (0.5 g DCW/L). All parameters were calculated when either more than 90% of xylose was consumed or fermented for up to 240 h. Acetate was not detected during the xylose fermentation.
Parameters: $Y_{Xylitol}$, Xylitol yield (g xylitol/g xylose); $Y_{Glycerol}$, Glycerol yield (g glycerol/g xylose); $Y_{Ethanol}$, Ethanol yield (g ethanol/g xylose); $P_{Ethanol}^{*}$, Specific ethanol productivity (g/g cell/h); *n. d.*, not detected.

https://doi.org/10.1371/journal.pone.0236294.t002

Table 3. Fermentation profiles of *S. cerevisiae* strains expressing the xylose isomerase pathway derived from *Orpinomyces* sp.

Name	Background	Genotype	Conditions	Initial cell (g DCW/L)	Xylose consumed (g/L)	Ethanol titer (g/L)	μ_{max}	r_{Xylose}	$Y_{Xylitol}$	$Y_{Ethanol}$	Reference
XYL123 *pho13Δ*	D452-2	*XYL1*, *XYL2*, *XYL3*, *ald6Δ*, *pho13Δ*	AN, YPX (40)	25.0	39.4	10.5	0.24	5.93	0.2	0.27	This study
XI-XYL3	D452-2	*xylA**, *XYL3*, *ald6Δ*	OL, YPX (40)	25.0	30.3	-	0.20	0.15	0.40	-	This study
			AN, YPX (40)	25.0	24.8	9.1	0.16	0.10	0.16	0.37	This study
XI-XYL3 *pho13Δ*	D452-2	*xylA**, *XYL3*, *ald6Δ*, *pho13Δ*	OL, YPX (40)	25.0	28.1	-	0.20	0.13	0.42	-	This study
			AN, YPX (40)	25.0	19.4	7.3	0.14	0.08	0.18	0.37	This study
YΔGP/XK/XI	YPH499	*xylA* (n = 15), *XKS1*, *gre3Δ*, *pho13Δ*	OL, YPX (50)	50 g wet cells/L	~50	~22.5	-	2.08	0.02	0.45	[39]
LVY34.4	LVYA1	*xylA** (n = 36), *gre3Δ*, *RPE1*, *RKI1*, *TKL1*, *TAL1*, 2×*XKS1*, Evolved	O, YPX(30)	0.25	< 30.0	< 13.8	0.21	1.32	0.005	0.46	[22]
ADAP8	INVSc1	*xylA*, *SUT1*, *XKS1*, Evolved	AN, YPX (20)	5.0	10.8	3.4	0.13	0.09	0.26	0.32	[40]
YCOA2E	NAPX37	*xylA**, *XKS1*, *HXT7*, *BGL1*, *GXS1*, *Δgre3*, *Δhxt16*, Evolved	OL, YPX (20)	0.05	16.6	6.7	0.09	1.66	-	0.41	[41]
O7E15	NAPX37	*xylA**(n = unknown), *XKS1*, *HXT7*, *BGL1*, *GXS1*, *Δgre3*, *Δhxt16*, Evolved	OL, YPX (40)	0.2	29.7	13.0	-	0.62	-	0.44	[42]

Parameters: *xylA**, codon optimized *Orpinomyces* sp. *xylA*, DCW, Dried cell weight; O, Oxygen conditions; OL, Oxygen-limited conditions; AN, Anaerobic conditions; μ_{max}, Volumetric growth rate (g/L-h); r_{Xylose}, Xylose consumption rate (g xylose/L/h); $Y_{Xylitol}$, Xylitol yield (g xylitol/g xylose); $Y_{Ethanol}$, Ethanol yield (g ethanol/g xylose).

https://doi.org/10.1371/journal.pone.0236294.t003

not inhibited up to 70 g/L xylose (Fig 3A), and it did not undergo adaptive evolutionary process until 65 generations (S3 Fig).

In the XI-XYL3 strain, however, the growth rate gradually increased up to 50 g/L xylose, and there was no initial growth observed at 100 g/L xylose (Fig 4B). At 40 g/L xylose, therefore, serial sub-cultures of the XI-XYL3 strain would not provide high selection pressure for better growers. In fact, until 110 generations, the culture of the XI-XYL3 strain did not show improvement in the growth rates (Fig 4C). At 100 g/L, meanwhile, serial sub-cultures of the XI-XYL3 strain did show slight improvement in the growth rates (Fig 4D); however, the isolated mutants did not have advantages in xylose fermentation (S1 and S4 Figs and S3 Table). Also, it was confirmed again that *pho13Δ* in the XI-XYL3 strain was not as critical as in the XYL123 strain regardless of xylose concentrations (Fig 4B), and during serial subcultures on 40 g/L and 100 g/L xylose (S3 Fig). Therefore, it was confirmed that either *pho13Δ* or evolutionary engineering could be an efficient strategy to improve strains expressing the xylose oxidoreductase pathway; however, the strategy of either *pho13Δ* or evolutionary engineering to improve strain expressing the xylose isomerase pathway did not have more dramatic results than the strain expressing the xylose oxidoreductase pathway.

Additional copies of *xylA* improves xylose consumption significantly

Several pathway-targeted approaches have been reported for the improvement of the xylose isomerase pathway (Table 3 and Fig 5A). First, the deletion of *GRE3* encoding aldose reductase and/or the deletion of *SOR1* encoding sorbitol (xylitol) dehydrogenase were proposed to

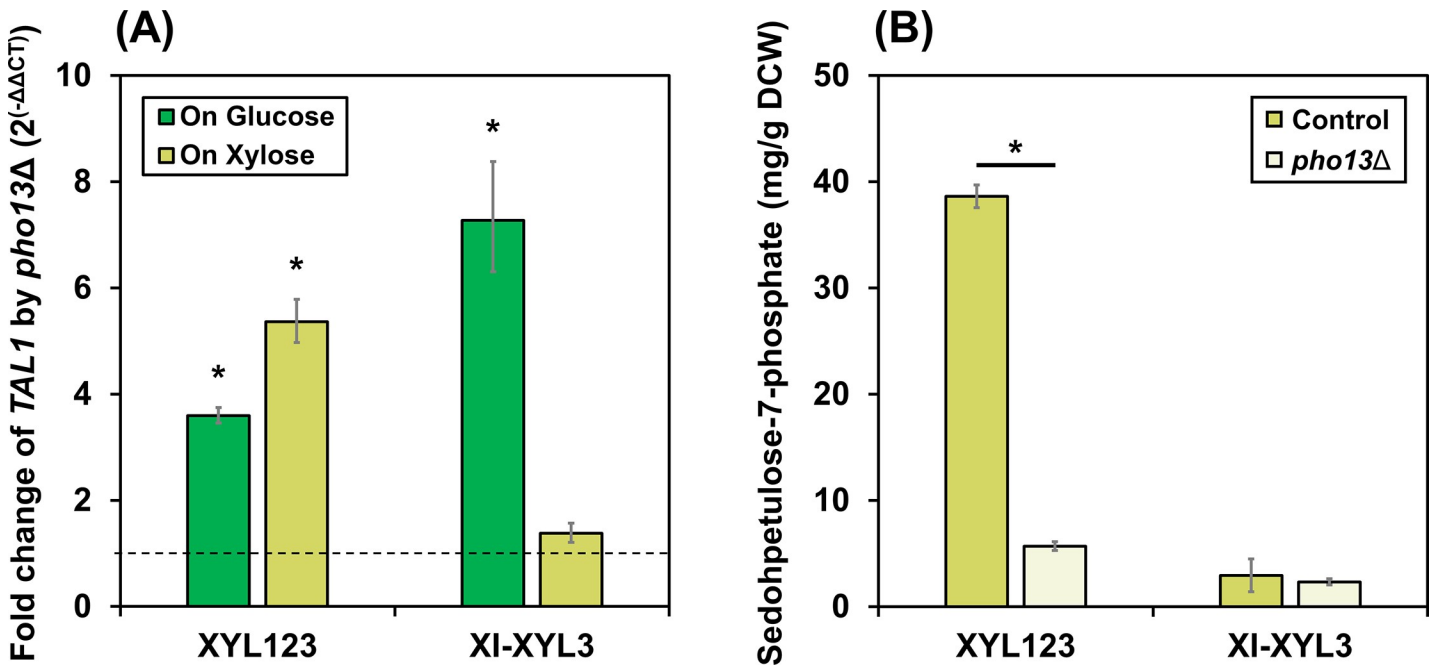

Fig 3. *PHO13* deletion-induced transcriptional and metabolic changes in two xylose-metabolizing strains. (A) Fold changes in the mRNA levels of the *TAL1* gene in the *pho13*Δ mutants of the XYL123 and the XI-XYL3 strains growing on glucose or xylose. The dashed line is 1, referring to the *PHO13* wild type. (B) The intracellular concentrations of sedeheptulose-7-phospahte in the *PHO13* wild types (control) and the *pho13*Δ mutants of the XYL123 and the XI-XYL3 strains growing on xylose. Asterisks denote statistically significant differences (Student's t-test, $p < 0.05$).

https://doi.org/10.1371/journal.pone.0236294.g003

reduce xylitol accumulation [45,46]. Also, extra copies of *xylA* and/or *XYL3* [22,39,42] were often accompanied with the overexpression of the PP pathway genes such as *TAL1* to improve xylose consumption rates. In Fig 5B, the necessity and contribution of each factors above were evaluated. Although some mutants showed statistically significant increases in growth rate and decreases in xylitol accumulation, none of the single factors contributed to ethanol production from xylose under oxygen-limited conditions (Table 2 and S3 Table). In fact, the most significant improvement was made by the expression of an additional copy of *xylA* in the $(XI)_2$-XYL3 strain with the xylose consumption rate of 0.10 g/L-h. When multiple copies of the *xylA* gene were integrated at δ sequences (Ty2 transposable element) (S5 Fig), one of the 26 resulting strains (δ(XI)-XYL3) was confirmed for the improved phenotypes (S6 Fig) and for the increased expression levels of the *xylA* gene (35-fold increase, S7 Fig). The δ(XI)-XYL3 strain showed the highest xylose consumption rate (0.15 g/L-h) with detectable amount of ethanol (Fig 5C and Table 2). In addition, with the improved level of xylose consumption, *pho13*Δ was shown to contribute to ethanol yield of the δ(XI)-XYL3 strain while its xylose consumption was not affected (Fig 5C, S6 Fig). However, the xylose consumption rate of the δ(XI)-XYL3 *pho13*Δ strain was still lower than that of the XYL123 *pho13*Δ strain (0.93 g/L-h) as well as those of the previously reported strains with 15–36 copies of the *xylA* gene (1.32–2.08 g/L-h, Table 3) [22,39]. The result suggested that the expression level of the *xylA* gene is one of the most critical factor for efficient xylose consumption, and the δ(XI)-XYL3 strain may have not reached to an optimal level of the *xylA* expression.

Discussion

There have been numerous attempts to develop *S. cerevisiae* strains fermenting xylose efficiently for decades [37,47,48]. Broadening the substrate range of *S. cerevisiae* is required not

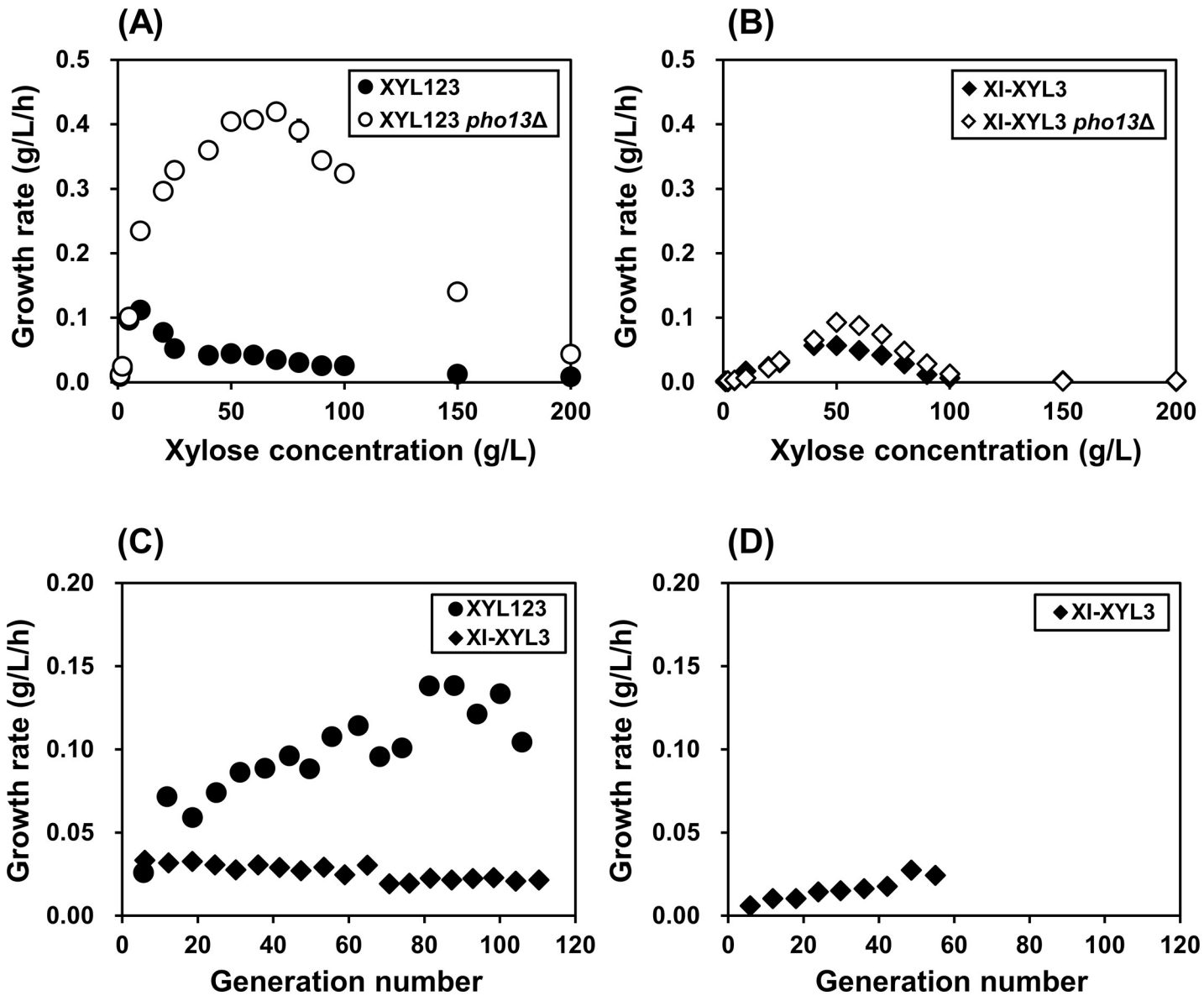

Fig 4. Adaptive evolution of two xylose-metabolizing strains on xylose. For adaptive evolution on xylose, growth rates of the XYL123 strains (A) and the XI-XYL3 strains (B) were evaluated under different xylose concentrations. Under growth-liming concentrations of xylose, 40 g/L (C) and 100 g/L (D), the strains were serially subcultured until the described generation numbers.

https://doi.org/10.1371/journal.pone.0236294.g004

only to support cellulosic bioprocesses but also to extend product spectrum and efficiency with alternative substrates other than glucose [26,49]. In fact, metabolic engineering for xylose fermentation is a preliminary step toward strain development for desired products. However, the approaches to design efficient *S. cerevisiae* strains expressing the xylose isomerase pathway varied greatly, and adaptive evolution was essential in most prior studies (Table 3) [11,13,20,22,50–52]. It is contradictory to the fact that the optimization of strains expressing the xylose oxidoreductase pathway can be reproducibly achieved by two factors: the constitutive expression of *XYL1*, *XYL2*, and *XYL3* from *P. stipitis* and the deletion of the *PHO13* gene (*pho13*Δ) [3]. Although a prior study presented a reduction in the lag phase by *pho13*Δ in the strain expressing the xylose isomerase pathway, the improvement was not as significant as

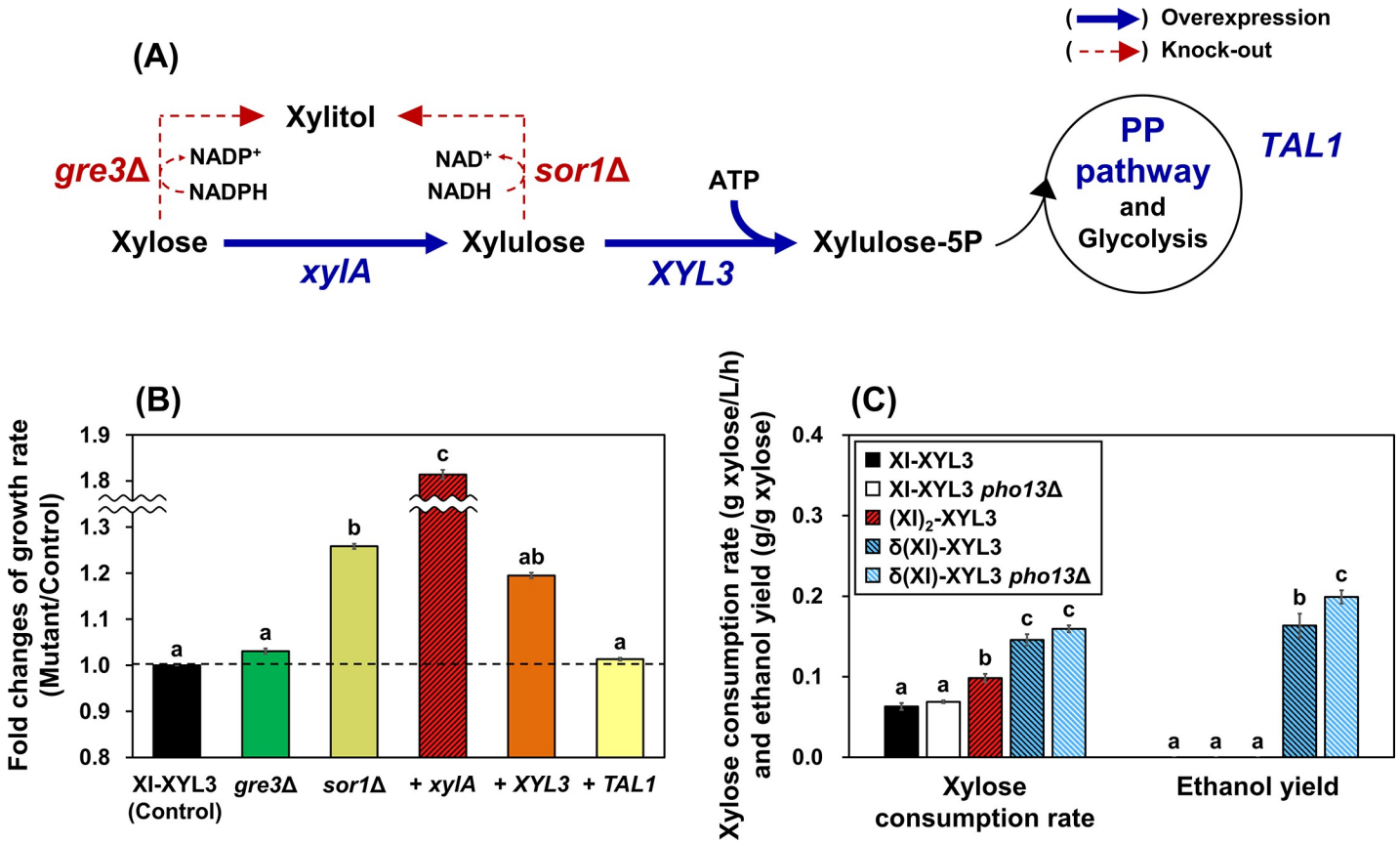

Fig 5. Pathway-targeted approaches to improve strains expressing the xylose isomerase pathway. (A) The target genes to be deleted (*gre3*Δ, *sor1*Δ) and the target genes to be overexpressed by integration of a duplicated copy (*xylA*, *XYL3*, *TAL1*). (B) Relative changes in growth rates (g/L-h) on xylose of the engineered strains compared to the XI-XYL3 strain. (C) Comparison of fermentation profiles of the XI-XYL3, $(XI)_2$-XYL3, and δ(XI)-XYL3 strains, and their *pho13*Δ mutants. All fermentations were performed in YP medium containing 40 g/L xylose under oxygen-limited conditions (80 rpm), with a low initial cell density (0.5 g DCW/L). Different letters represent significant differences across strains within fermentation parameters (Tukey's test, $p < 0.05$). *n. d.*; Not detected.

https://doi.org/10.1371/journal.pone.0236294.g005

those achieved by adaptive evolution in the same study [11]. The other study, which reported an 8% increase in the ethanol yield by *pho13*Δ in the xylose isomerase strain, used an extreme condition with an initial OD of 40 [39]. Consistent with previous findings, we also found that *pho13*Δ improved ethanol yield but it was only in the strain expressing multiple copies of *xylA* but not in the single copy *xylA* strain (Fig 5). Also, the xylose consumption rate remained constant in both strains, suggesting the conditional and limited effect of *pho13*Δ in the xylose isomerase strains.

One of the most recent studies reported that nine different expression cassettes of *Piromyces* sp. *xylA*, the overexpression of both *XKS1* and six non-oxidative PP genes (*RPE1*, *RKI1*, *TAL1*, *NQM1*, *TKL1*, *TKL2*), and deletion of the *GRE3* gene are required to construct a xylose-assimilating *S. cerevisiae* strain [50]. The resulting strain was able to produce ethanol after adaptive evolution, in which the loss of function mutation in the *PMR1* gene was critical [50]. In another recent study, two copies of a mutant version of *Piromyces* sp. *xylA* (E15D, E114G, E129D, T142S, A177T, and V433I), the overexpression of *XKS1* and *TAL1*, *pho13*Δ and *GRE3* as well as laboratory evolution were required for xylose fermentation [51,52]. The study concluded that the laboratory evolution was partially contributed by the loss of function mutations in the *PMR1* and *ASC1* genes [51]. Although the metabolic engineering approaches are complicated and different between the two studies, the studies shared the idea that the xylose

isomerase step is the most limiting; therefore, 1) either multiple integration or protein engineering of xylose isomerase is required, and 2) the homeostasis of its inorganic cofactor has to be modified (*pmr1*Δ). The expression of approximately 36 copies of *Orpinomyces sp*. *xylA* [22] and the mutation in *ASK10* for proper folding of isomerase [20] were also proposed to overcome the limitation in xylose isomerase. The above results from recent studies are all consistent with the findings of the present study that the copy number increase in the xylose isomerase gene is the most critical and primarily required (Table 3). However, the optimal level of the copy number of the *xylA* gene varies greatly among studies with the same *xylA* gene derived from *Orpinomyces* sp (Table 3).

It should be noted that the comparison of the two pathways in the present study was limited to the genes originated from *P*. *stipitis* and *Orpinomyces* sp. for the oxidoreductase and the isomerase pathways, respectively. Considering that the *xylA* gene was originated from strictly anaerobic fungus *Orpinomyces* sp., its functional expression in yeast could have been limited compared to other *xylA* genes originated from bacteria and other fungi [53]. Also, we only compared fermentation properties under oxygen-limited conditions with a low initial cell density. Indeed, under anaerobic conditions with a high initial cell density, where the limited growth of the XI-XYL3 strain can be compensated, the XI-XYL3 strain could produce ethanol at a higher yield (0.37 g/g xylose) than those achieved in the XYL123 strain (0.27 g/g xylose) (Table 3). Nevertheless, engineering an efficient xylose-fermenting strain using the xylose isomerase pathway remains challenging because of the difficulties in reproducing adaptive evolution successfully and achieving optimal copy numbers of the *xylA* gene, as previously reported.

The present study aimed to develop a simple method to optimize *S*. *cerevisiae* expressing the xylose isomerase pathway: a genome-integrated heterologous xylose isomerase gene (*xylA*) under a strong promoter. We found that adaptive evolution as well as some of the pathway-targeted approaches (*gre3*Δ, *XYL3*, *TAL1*) did not work as efficiently as previously reported. One the other hand, significant improvement in xylose fermentation was achieved by *sor1*Δ as well as multiple integration of the *xylA* gene with or without *pho13*Δ. However, the improved strain was still inferior to an isogenic strain expressing xylose oxidoreductase pathway: xylose reductase (*XYL1*) and xylitol dehydrogenase (*XYL2*). Because the above mentioned approaches for the xylose isomerase pathway were successfully demonstrated in other studies, we think that other unknown factors are required such as different source of the *xylA* gene [53,54], different strain backgrounds [55,56], and/or other metabolic engineering designs. Although recent studies successfully discovered several knockout targets (*ISU1*, *HOG1*, *GRE3*, *IRA2*, *SSK2*) to improve the xylose isomerase pathway, they still required a strain background with the overexpression of the genes in the pentose phosphate pathway and/or the expression of multiple copies of the *xylA* gene [22,24]. With the current level of knowledge regarding xylose isomerase and its functional expression in *S*. *cerevisiae*, therefore, the xylose oxidoreductase pathway provides a more reproducible strategy to engineer xylose-fermenting strains.

Supporting information

S1 Text. Supplementary materials and methods.
(DOCX)

S1 Fig. Growth rate comparison of the evolved colonies of the XYL123 (A), XI-XYL3 (B), and XI-XYL3 *pho13*Δ (C) strains. Two-three most promising colonies were selected from each group, and denoted to XYL123e, XI-XYL3e, and XI-XYL3 *pho13*Δe, respectively. Strains were cultured in YP medium containing either 40 g/L xylose (A) or 100 g/L xylose (B, C) under oxygen-limited conditions (80 rpm). Volumetric growth rates were calculated at the exponential

phase.
(TIF)

S2 Fig. Fermentation profiles of the evolved strains expressing the xylose oxidoreductase pathway (the XYL123e strains). The XYL123 and XYL123 *pho13*Δ strains were used as the controls. Cell density (A), xylose concentrations (B), and fermentation parameters (C) were compared. Fermentations were performed in YP medium containing 40 g/L xylose under oxygen-limited conditions (80 rpm) with a starting OD_{600} of 1.0. Different letters (*a*, *b*, and *c*) represent significant differences ($p < 0.05$, ANOVA method). *n*. *d*.; Not detected.
(TIF)

S3 Fig. Adaptive evolution of the *pho13*Δ mutants of the XYL123 and the XI-XYL3 strains on xylose. Under growth-liming concentrations of xylose, 40 g/L (A) and 100 g/L (A), the strains were serially subcultured until the described generation numbers.
(TIF)

S4 Fig. Fermentation profiles of the evolved *S. cerevisiae* strains expressing the isomerase pathway on 100 g/L xylose fermentation. (A, B, C) The XI-XYL3 strain and its evolved strains (XI-XYL3e1, XI-XYL3e2). (C, D, E) The XI-XYL3 *pho13*Δ strain and its evolved strains (XI-XYL3 *pho13*Δe1, XI-XYL3 *pho13*Δe2). The strains were evaluated in YP medium containing 40 g/L xylose under oxygen-limited conditions (80 rpm) with a starting OD_{600} of 1.0. Different letters (*a*, *b*, and *c*) represent significant differences ($p < 0.05$, ANOVA method). *n*. *d*.; Not detected.
(TIF)

S5 Fig. Fermentation profiles of 26 mutants overexpressing the *xylA* gene by δ-integration on xylose fermentation. The XI-XYL3 strain and 26 mutants were evaluated the consumed xylose (g/L) (A) and the produced ethanol (g/L) (B) under oxygen-limited conditions (80 rpm). Six-mutants, which can produce ethanol, were selected and evaluated the xylose consumption rate (g xylose/L/h) and ethanol yield (g ethanol/g xylose) under oxygen-limited conditions (C) and anaerobic conditions (D). Fermentations were performed in YP medium containing 40 g/L xylose, with a starting OD_{600} of 1.0. The dashed line refer to the XI-XYL3 strain.
(TIF)

S6 Fig. Fermentation profiles of the XI-XYL3, δ(XI)-XYL3 and δ(XI)-XYL3 *pho13*Δ strains on 40 g/L xylose fermentation under two different oxygen conditions. The strains were evaluated in YP medium containing 40 g/L xylose under oxygen-limited conditions (80 rpm, A-C) and anaerobic condition (D-F) with a starting OD_{600} of 1.0.
(TIF)

S7 Fig. Comparison of transcriptional levels of *xylA* gene increased by δ-integration in two xylose isomerase pathway strains (XI-XYL3 and δ(XI)-XYL3 strains). Increased transcriptional levels of the *xylA* gene in the XI-XYL3 and the *xylA* overexpressed strain (δ(XI)-XYL3) by δ-integration was confirmed by RT-qPCR. Fermentations were performed in YP medium containing 40 g/L (YPX40) or 100 g/L (YPX100) xylose, with a starting OD_{600} of 1.0. Asterisks denote statistically significant differences (Student's t-test, $p < 0.05$).
(TIF)

S1 Table. Plasmids used in this study.
(DOCX)

S2 Table. Primers and guide RNAs used in this study.
(DOCX)

S3 Table. Fermentation profiles of evolved *S. cerevisiae* expressing the xylose oxidoreductase pathway.
(DOCX)

Author Contributions

Conceptualization: Deokyeol Jeong, Eun Jung Lee, Soo Rin Kim.

Data curation: Deokyeol Jeong.

Formal analysis: Deokyeol Jeong, Eun Joong Oh, Soo Rin Kim.

Funding acquisition: Eun Jung Lee, Soo Rin Kim.

Investigation: Deokyeol Jeong, Eun Jung Lee, Soo Rin Kim.

Methodology: Deokyeol Jeong, Soo Rin Kim.

Resources: Soo Rin Kim.

Supervision: Soo Rin Kim.

Validation: Deokyeol Jeong, Eun Joong Oh, Soo Rin Kim.

Writing – original draft: Deokyeol Jeong, Eun Joong Oh, Eun Jung Lee, Soo Rin Kim.

Writing – review & editing: Deokyeol Jeong, Eun Joong Oh, Ja Kyong Ko, Ju-Ock Nam, Hee-Soo Park, Yong-Su Jin, Eun Jung Lee, Soo Rin Kim.

References

1. Cox PM, Betts RA, Jones CD, Spall SA, Totterdell IJ (2000) Acceleration of global warming due to carbon-cycle feedbacks in a coupled climate model. Nature 408: 184. https://doi.org/10.1038/35041539 PMID: 11089968
2. Mosier N, Wyman C, Dale B, Elander R, Lee YY, et al. (2005) Features of promising technologies for pretreatment of lignocellulosic biomass. Bioresource technology 96: 673–686. https://doi.org/10.1016/j.biortech.2004.06.025 PMID: 15588770
3. Kim SR, Skerker JM, Kang W, Lesmana A, Wei N, et al. (2013) Rational and evolutionary engineering approaches uncover a small set of genetic changes efficient for rapid xylose fermentation in *Saccharomyces cerevisiae*. PloS one 8: e57048. https://doi.org/10.1371/journal.pone.0057048 PMID: 23468911
4. Banerjee S, Mishra G, Roy A (2019) Metabolic engineering of bacteria for renewable bioethanol production from cellulosic biomass. Biotechnology and Bioprocess Engineering 24: 713–733.
5. Hahn-Hagerdal B, Karhumaa K, Jeppsson M, Gorwa-Grauslund MF (2007) Metabolic engineering for pentose utilization in *Saccharomyces cerevisiae*. Advances in biochemical engineering/biotechnology 108: 147–177. https://doi.org/10.1007/10_2007_062 PMID: 17846723
6. Cai Z, Zhang B, Li Y (2012) Engineering *Saccharomyces cerevisiae* for efficient anaerobic xylose fermentation: Reflections and perspectives. Biotechnology Journal 7: 34–46. https://doi.org/10.1002/biot.201100053 PMID: 22147620
7. Li X, Park A, Estrela R, Kim SR, Jin YS, et al. (2016) Comparison of xylose fermentation by two high-performance engineered strains of *Saccharomyces cerevisiae*. Biotechnology reports 9: 53–56. https://doi.org/10.1016/j.btre.2016.01.003 PMID: 28352592
8. Karhumaa K, Garcia Sanchez R, Hahn-Hägerdal B, Gorwa-Grauslund M-F (2007) Comparison of the xylose reductase-xylitol dehydrogenase and the xylose isomerase pathways for xylose fermentation by recombinant *Saccharomyces cerevisiae*. Microbial cell factories 6: 5–5. https://doi.org/10.1186/1475-2859-6-5 PMID: 17280608
9. Sonderegger M, Sauer U (2003) Evolutionary engineering of *Saccharomyces cerevisiae* for anaerobic growth on xylose. Applied and Environmental Microbiology 69: 1990–1998. https://doi.org/10.1128/aem.69.4.1990-1998.2003 PMID: 12676674

10. Scalcinati G, Otero JM, Van Vleet JRH, Jeffries TW, Olsson L, et al. (2012) Evolutionary engineering of *Saccharomyces cerevisiae* for efficient aerobic xylose consumption. FEMS Yeast Research 12: 582–597. https://doi.org/10.1111/j.1567-1364.2012.00808.x PMID: 22487265

11. Lee S-M, Jellison T, Alper HS (2014) Systematic and evolutionary engineering of a xylose isomerase-based pathway in *Saccharomyces cerevisiae* for efficient conversion yields. Biotechnology for biofuels 7: 122. https://doi.org/10.1186/s13068-014-0122-x PMID: 25170344

12. Shen Y, Chen X, Peng B, Chen L, Hou J, et al. (2012) An efficient xylose-fermenting recombinant *Saccharomyces cerevisiae* strain obtained through adaptive evolution and its global transcription profile. Applied Microbiology and Biotechnology 96: 1079–1091. https://doi.org/10.1007/s00253-012-4418-0 PMID: 23053078

13. Zhou H, Cheng JS, Wang BL, Fink GR, Stephanopoulos G (2012) Xylose isomerase overexpression along with engineering of the pentose phosphate pathway and evolutionary engineering enable rapid xylose utilization and ethanol production by *Saccharomyces cerevisiae*. Metabolic Engineering 14: 611–622. https://doi.org/10.1016/j.ymben.2012.07.011 PMID: 22921355

14. Van Vleet JH, Jeffries TW, Olsson L (2008) Deleting the para-nitrophenyl phosphatase (pNPPase), PHO13, in recombinant Saccharomyces cerevisiae improves growth and ethanol production on D-xylose. Metabolic Engineering 10: 360–369. https://doi.org/10.1016/j.ymben.2007.12.002 PMID: 18249574

15. Ni H, Laplaza JM, Jeffries TW (2007) Transposon mutagenesis to improve the growth of recombinant *Saccharomyces cerevisiae* on D-xylose. Appl Environ Microbiol 73: 2061–2066. https://doi.org/10.1128/AEM.02564-06 PMID: 17277207

16. Fujitomi K, Sanda T, Hasunuma T, Kondo A (2012) Deletion of the *PHO13* gene in *Saccharomyces cerevisiae* improves ethanol production from lignocellulosic hydrolysate in the presence of acetic and formic acids, and furfural. Bioresource technology 111: 161–166. https://doi.org/10.1016/j.biortech.2012.01.161 PMID: 22357292

17. Xu H, Kim S, Sorek H, Lee Y, Jeong D, et al. (2016) *PHO13* deletion-induced transcriptional activation prevents sedoheptulose accumulation during xylose metabolism in engineered *Saccharomyces cerevisiae*. Metabolic Engineering 34: 88–96. https://doi.org/10.1016/j.ymben.2015.12.007 PMID: 26724864

18. Kim SR, Xu H, Lesmana A, Kuzmanovic U, Au M, et al. (2015) Deletion of *PHO13*, encoding haloacid dehalogenase type IIA phosphatase, results in upregulation of the pentose phosphate pathway in *Saccharomyces cerevisiae*. Applied and Environmental Microbiology 81: 1601–1609. https://doi.org/10.1128/AEM.03474-14 PMID: 25527558

19. Ko JK, Um Y, Lee SM (2016) Effect of manganese ions on ethanol fermentation by xylose isomerase expressing *Saccharomyces cerevisiae* under acetic acid stress. Bioresource technology 222: 422–430. https://doi.org/10.1016/j.biortech.2016.09.130 PMID: 27744166

20. Hou J, Jiao C, Peng B, Shen Y, Bao X (2016) Mutation of a regulator Ask10p improves xylose isomerase activity through up-regulation of molecular chaperones in *Saccharomyces cerevisiae*. Metabolic Engineering 38: 241–250. https://doi.org/10.1016/j.ymben.2016.08.001 PMID: 27497973

21. Reider Apel A, d'Espaux L, Wehrs M, Sachs D, Li RA, et al. (2016) A Cas9-based toolkit to program gene expression in *Saccharomyces cerevisiae*. Nucleic acids research 45: 496–508. https://doi.org/10.1093/nar/gkw1023 PMID: 27899650

22. dos Santos LV, Carazzolle MF, Nagamatsu ST, Sampaio NMV, Almeida LD, et al. (2016) Unraveling the genetic basis of xylose consumption in engineered *Saccharomyces cerevisiae* strains. Scientific Reports 6: 38676. https://doi.org/10.1038/srep38676 PMID: 28000736

23. Parreiras LS, Breuer RJ, Narasimhan RA, Higbee AJ, La Reau A, et al. (2014) Engineering and two-stage evolution of a lignocellulosic hydrolysate-tolerant *Saccharomyces cerevisiae* strain for anaerobic fermentation of xylose from AFEX pretreated corn stover. PloS one 9: e107499. https://doi.org/10.1371/journal.pone.0107499 PMID: 25222864

24. Sato TK, Tremaine M, Parreiras LS, Hebert AS, Myers KS, et al. (2016) Directed evolution reveals unexpected epistatic interactions that alter metabolic regulation and enable anaerobic xylose use by *Saccharomyces cerevisiae*. PLoS genetics 12: e1006372. https://doi.org/10.1371/journal.pgen.1006372 PMID: 27741250

25. Ye S, Jeong D, Shon JC, Liu K-H, Kim KH, et al. (2019) Deletion of *PHO13* improves aerobic l-arabinose fermentation in engineered *Saccharomyces cerevisiae*. Journal of Industrial Microbiology & Biotechnology 46: 1725–1731.

26. Jeong D, Ye S, Park H, Kim SR (2020) Simultaneous fermentation of galacturonic acid and five-carbon sugars by engineered *Saccharomyces cerevisiae*. Bioresource Technology 295: 122259. https://doi.org/10.1016/j.biortech.2019.122259 PMID: 31639627

27. Hosaka K, Nikawa J-i, Kodaki T, Yamashita S (1992) A dominant mutation that alters the regulation of *INO1* expression in *Saccharomyces cerevisiae*. The Journal of Biochemistry 111: 352–358. https://doi.org/10.1093/oxfordjournals.jbchem.a123761 PMID: 1587797

28. Kim SR, Ha S-J, Kong II, Jin Y-S (2012) High expression of *XYL2* coding for xylitol dehydrogenase is necessary for efficient xylose fermentation by engineered *Saccharomyces cerevisiae*. Metabolic Engineering 14: 336–343. https://doi.org/10.1016/j.ymben.2012.04.001 PMID: 22521925

29. Kim S, Lee DY, Wohlgemuth G, Park HS, Fiehn O, et al. (2013) Evaluation and optimization of metabolome sample preparation methods for *Saccharomyces cerevisiae*. Analytical chemistry 85: 2169–2176. https://doi.org/10.1021/ac302881e PMID: 23289506

30. Hector RE, Dien BS, Cotta MA, Mertens JA (2013) Growth and fermentation of D-xylose by *Saccharomyces cerevisiae* expressing a novel D-xylose isomerase originating from the bacterium *Prevotella ruminicola* TC2-24. Biotechnology for biofuels 6: 84. https://doi.org/10.1186/1754-6834-6-84 PMID: 23721368

31. Kim B, Du J, Eriksen DT, Zhao H (2013) Combinatorial design of a highly efficient xylose-utilizing pathway in *Saccharomyces cerevisiae* for the production of cellulosic biofuels. Applied and Environmental Microbiology 79: 931–941. https://doi.org/10.1128/AEM.02736-12 PMID: 23183982

32. Saint-Prix F, Bönquist L, Dequin S (2004) Functional analysis of the *ALD* gene family of *Saccharomyces cerevisiae* during anaerobic growth on glucose: the NADP+-dependent Ald6p and Ald5p isoforms play a major role in acetate formation. Microbiology 150: 2209–2220. https://doi.org/10.1099/mic.0.26999-0 PMID: 15256563

33. Bellissimi E, van Dijken JP, Pronk JT, van Maris AJA (2009) Effects of acetic acid on the kinetics of xylose fermentation by an engineered, xylose-isomerase-based *Saccharomyces cerevisiae* strain. FEMS Yeast Research 9: 358–364. https://doi.org/10.1111/j.1567-1364.2009.00487.x PMID: 19416101

34. Ko JK, Um Y, Lee S-M (2016) Effect of manganese ions on ethanol fermentation by xylose isomerase expressing *Saccharomyces cerevisiae* under acetic acid stress. Bioresource Technology 222: 422–430. https://doi.org/10.1016/j.biortech.2016.09.130 PMID: 27744166

35. Sonderegger M, Schümperli M, Sauer U (2004) Metabolic engineering of a phosphoketolase pathway for pentose catabolism in *Saccharomyces cerevisiae*. Applied and environmental microbiology 70: 2892–2897. https://doi.org/10.1128/aem.70.5.2892-2897.2004 PMID: 15128548

36. Zhang Y, Lane S, Chen J-M, Hammer SK, Luttinger J, et al. (2019) Xylose utilization stimulates mitochondrial production of isobutanol and 2-methyl-1-butanol in *Saccharomyces cerevisiae*. Biotechnology for Biofuels 12: 223. https://doi.org/10.1186/s13068-019-1560-2 PMID: 31548865

37. Kim SR, Park Y-C, Jin Y-S, Seo J-H (2013) Strain engineering of *Saccharomyces cerevisiae* for enhanced xylose metabolism. Biotechnology advances 31: 851–861. https://doi.org/10.1016/j.biotechadv.2013.03.004 PMID: 23524005

38. Kim SR, Kwee NR, Kim H, Jin Y-S (2013) Feasibility of xylose fermentation by engineered Saccharomyces cerevisiae overexpressing endogenous aldose reductase (*GRE3*), xylitol dehydrogenase (*XYL2*), and xylulokinase (*XYL3*) from *Scheffersomyces stipitis*. FEMS Yeast Research 13: 312–321. https://doi.org/10.1111/1567-1364.12036 PMID: 23398717

39. Bamba T, Hasunuma T, Kondo A (2016) Disruption of *PHO13* improves ethanol production via the xylose isomerase pathway. AMB Express 6: 4. https://doi.org/10.1186/s13568-015-0175-7 PMID: 26769491

40. Madhavan A, Tamalampudi S, Srivastava A, Fukuda H, Bisaria VS, et al. (2009) Alcoholic fermentation of xylose and mixed sugars using recombinant *Saccharomyces cerevisiae* engineered for xylose utilization. Applied Microbiology and Biotechnology 82: 1037–1047. https://doi.org/10.1007/s00253-008-1818-2 PMID: 19125247

41. Li YC, Li GY, Gou M, Xia ZY, Tang YQ, et al. (2016) Functional expression of xylose isomerase in flocculating industrial *Saccharomyces cerevisiae* strain for bioethanol production. Journal of Bioscience and Bioengineering 121: 685–691. https://doi.org/10.1016/j.jbiosc.2015.10.013 PMID: 26645659

42. Li YC, Zeng WY, Gou M, Sun ZY, Xia ZY, et al. (2017) Transcriptome changes in adaptive evolution of xylose-fermenting industrial *Saccharomyces cerevisiae* strains with delta-integration of different *xylA* genes. Applied Microbiology and Biotechnology 101: 7741–7753. https://doi.org/10.1007/s00253-017-8494-z PMID: 28900684

43. Kobayashi Y, Sahara T, Suzuki T, Kamachi S, Matsushika A, et al. (2017) Genetic improvement of xylose metabolism by enhancing the expression of pentose phosphate pathway genes in *Saccharomyces cerevisiae* IR-2 for high-temperature ethanol production. Journal of Industrial Microbiology & Biotechnology 44: 879–891.

44. Lian J, Bao Z, Hu S, Zhao H (2018) Engineered CRISPR/Cas9 system for multiplex genome engineering of polyploid industrial yeast strains. Biotechnology and bioengineering 115: 1630–1635. https://doi.org/10.1002/bit.26569 PMID: 29460422

45. Traff KL, Otero Cordero RR, van Zyl WH, Hahn-Hagerdal B (2001) Deletion of the *GRE3* aldose reductase gene and its influence on xylose metabolism in recombinant strains of *Saccharomyces cerevisiae* expressing the *xylA* and *XKS1* genes. Applied and Environmental Microbiology 67: 5668–5674. https://doi.org/10.1128/AEM.67.12.5668-5674.2001 PMID: 11722921

46. Toivari MH, Salusjärvi L, Ruohonen L, Penttilä M (2004) Endogenous xylose pathway in *Saccharomyces cerevisiae*. Applied and Environmental Microbiology 70: 3681–3686. https://doi.org/10.1128/AEM.70.6.3681-3686.2004 PMID: 15184173

47. Li X, Chen Y, Nielsen J (2019) Harnessing xylose pathways for biofuels production. Current Opinion in Biotechnology 57: 56–65. https://doi.org/10.1016/j.copbio.2019.01.006 PMID: 30785001

48. Kwak S, Jo JH, Yun EJ, Jin Y-S, Seo J-H (2018) Production of biofuels and chemicals from xylose using native and engineered yeast strains. Biotechnology advances.

49. Kwak S, Jin Y-S (2017) Production of fuels and chemicals from xylose by engineered *Saccharomyces cerevisiae*: a review and perspective. Microbial cell factories 16: 82. https://doi.org/10.1186/s12934-017-0694-9 PMID: 28494761

50. Verhoeven MD, Lee M, Kamoen L, van den Broek M, Janssen DB, et al. (2017) Mutations in *PMR1* stimulate xylose isomerase activity and anaerobic growth on xylose of engineered *Saccharomyces cerevisiae* by influencing manganese homeostasis. Scientific Reports 7: 46155. https://doi.org/10.1038/srep46155 PMID: 28401919

51. Tran Nguyen Hoang P, Ko JK, Gong G, Um Y, Lee S-M (2018) Genomic and phenotypic characterization of a refactored xylose-utilizing *Saccharomyces cerevisiae* strain for lignocellulosic biofuel production. Biotechnology for biofuels 11: 268. https://doi.org/10.1186/s13068-018-1269-7 PMID: 30288173

52. Lee SM, Jellison T, Alper HS (2012) Directed evolution of xylose isomerase for improved xylose catabolism and fermentation in the yeast *Saccharomyces cerevisiae*. Applied and Environmental Microbiology 78: 5708–5716. https://doi.org/10.1128/AEM.01419-12 PMID: 22685138

53. Brat D, Boles E, Wiedemann B (2009) Functional expression of a bacterial xylose isomerase in *Saccharomyces cerevisiae*. Applied and environmental microbiology 75 8: 2304–2311. https://doi.org/10.1128/AEM.02522-08 PMID: 19218403

54. Seike T, Kobayashi Y, Sahara T, Ohgiya S, Kamagata Y, et al. (2019) Molecular evolutionary engineering of xylose isomerase to improve its catalytic activity and performance of micro-aerobic glucose/xylose co-fermentation in *Saccharomyces cerevisiae*. Biotechnology for Biofuels 12: 139. https://doi.org/10.1186/s13068-019-1474-z PMID: 31178927

55. Feng Q, Liu ZL, Weber SA, Li S (2018) Signature pathway expression of xylose utilization in the genetically engineered industrial yeast *Saccharomyces cerevisiae*. PloS one 13: e0195633. https://doi.org/10.1371/journal.pone.0195633 PMID: 29621349

56. Cunha JT, Soares PO, Romaní A, Thevelein JM, Domingues L (2019) Xylose fermentation efficiency of industrial *Saccharomyces cerevisiae* yeast with separate or combined xylose reductase/xylitol dehydrogenase and xylose isomerase pathways. Biotechnology for Biofuels 12: 20. https://doi.org/10.1186/s13068-019-1360-8 PMID: 30705706